



# Tectonic Setting of Metabasites of the Neo-Tethyan Oceanic Remains in Sanandaj-Sirjan Structural Zone, West of Isfahan, Central Iran

Ali-Khan Nasr-Esfahani\*

Geology department, Islamic Azad University, Khorasgan (Isfahan) Branch, Iran.

Received 25 March 2012; accepted 29 September 2012

## Abstract

The study area is located in the western portion of Isfahan, in Shahrekord-Dehsard Terrene. This area is part of the Sanandaj-Sirjan structural Zone. In this area, metamorphosed igneous outcrops contain greenschist and metabasite rocks. These rocks have metamorphosed into greenschist facies and belong to the Triassic-Jurassic age. The Metabasite is mainly composed of plagioclase, amphibole, epidote and chlorite. Geochemical data shows that the parent rocks are of basalt to andesitic basalt composition with sub alkaline and tholeiitic trends. In the REE and trace elements spider diagrams, these are similar to MORB and adapted with E-MORB. These results indicate a metabasite generated back arc basin volcanic subduction environment. The Metabasite in Sahrekord - Dehsard terrene shows remnants of a Neo-Tethyan oceanic lithosphere with a back arc basin environment that was subducted and uplifted to the surface.

**Keywords:** Metabasite, Neo-Tethyan, Petrology, Sanandaj-Sirjan.

## Introduction

The Zagros orogen as a part of the Alpine-Himalaya mountain chain is a well-defined active doubly-vergent and asymmetric orogenic belt [1] and extends in a northwest-southeast direction for about 2000 km from Taurus Mountain in southeastern Turkey to the Bandar-Abas syntax in southern Iran (Arfania and Shahriari, 2009). This orogenic belt (Fig. 1) consists of four NW-SE trending parallel zones: (1) Urumieh-Dokhtar Magmatic Arc (UDMA); (2) Sanandaj-Sirjan Zone (SSZ); (3) High Zagros; and (4) Zagros Simply Folded Belt (ZSFB). The Sanandaj-Sirjan Zone (SSZ) is a narrow zone of highly deformed rocks located between the towns of Sirjan in the southeast, and Sanandaj in the northwest [2]. The Sanandaj-Sirjan Zone is a metamorphic belt (greenschist amphibolite facies) that was exhumed during the Cretaceous - Tertiary continental collision between the Afro-Arabian continent and the Iranian plateau (e.g., Sengor and Natalin [3], Mohajjel and Fergusson [2]; Mohajjel et al. [4]. The rocks in this zone are the most highly deformed in the Zagros orogen and share the NW-SE trend of its structures. The Sanandaj-Sirjan Zone is thrust over the Arabian Platform along the Main Zagros Fault, which is marked at the surface by a discontinuous belt of ophiolitic rocks and mélanges running along the entire length of the orogen [5].

The Main Zagros Fault is deeply rooted and coincides with the suture between the Arabian Plate and Sanandaj-Sirjan Zone [6-7]. The Zagros Fold-Thrust Belt is a result of a total shortening of 65-78 km across the Zagros sedimentary basin from the Early Miocene onwards [8]. The basin is characterized by a sequence of sedimentary rocks up to 12 km thick including Paleozoic and Mesozoic shelf sediments and Cenozoic syn-orogenic strata that were deposited on the subsiding northeastern Arabian continental margin. In the Golpaygan area, the Sanandaj-Sirjan Zone can be subdivided into two parts: (i) southeastern part consisting of Jurassic metamorphosed rocks; and (ii) northwestern part, deformed in the Late Cretaceous, containing many intrusive felsic rocks [9]. The southeastern Sanandaj-Sirjan Zone is subdivided transversally into two separate regions: (i) northeastern region (Esfahan-Sirjan Block) consisting of Paleozoic, Mesozoic, and Cenozoic sedimentary rocks with typical Central Iranian stratigraphic features; and (ii) southwestern region (Shahrekord-Dehsard Terrane), which is an intensely faulted zone consisting of high- to low-grade metamorphic rocks and metasedimentary strata with intercalations of intermediate to basic volcanic rock. This terrene has been regarded as an old Precambrian basement [10], reactivated in the course of the Mesozoic Cimmerian Orogeny [11]. The boundary separating the southwest and the northeast regions is a major fault which Taraz [10] was the first to name as the Main Deep Fault. The Study area is situated in the Shahrekord-Dehsard terrain.

\*Corresponding author.

E-mail address (es): ali.nasr21@gmail.com

This sub-zone is distinguished from the other sub-zones by the abundance of metamorphic rocks. These rocks metamorphosed in greenschist facies and are of Triassic to Jurassic age (Fig. 2).

Schist, marble, amphibolite, quartzite, meta dolomite, and metasandstone are the main constituents. The Metamorphic conditions of these rocks are not well constrained. Earlier reports of Hercynian and older orogenies in Paleozoic rocks of the southeast Complexly Deformed Sub-zone have been disputed by Alavi [12] and most of the orogenic activity in the Sanandaj-Sirjan Zone is now related to closing of the Tethys. A large part of the Complexly Deformed Sub-zone consists of metamorphosed Mesozoic clastic, carbonate and some volcanic rocks. Subduction of Tethys under the marginal and Complexly Deformed Sub-zones has occurred to form a continental margin magmatic arc (Urumieh-Dokhtar Magmatic Arc) and associated plutonism, deformation and metamorphism [13]. The studied area is a large-scale ductile shear zone trending NW–SE nearly parallel to the Main Zagros Reverse. Rocks here have undergone

mylonitization causing mylonitic foliation and lineation. This area is characterized by the predominance of metamorphic rocks of both sedimentary and magmatic origins that are intruded by deformed granitoid bodies. The metamorphic rocks are of the Triassic-Jurassic age and constitute an assemblage of low grade metamorphic that has been affected by several tectono-metamorphic events [14]. Davoudian et al. [15] reported eclogites and other metamorphosed volcanic rocks in northern Shahrekord. They suggest that these rocks represent relics of the Neo-Tethys oceanic plate, which was subducted under the Iranian microcontinent. This area is near northern Shahrekord and geologically, the two regions are similar. In the study area, metamorphic rocks are dominated by paragneisses, greenschists, metabasites, meta carbonates, which are intruded by granites [13]. The metabasites are important metamorphic rocks which are assumed to be oceanic plate remains, these rocks are the focus of the present study, and may reveal important information on tectonic setting of the Sanandaj-Sirjan Zone in this area.

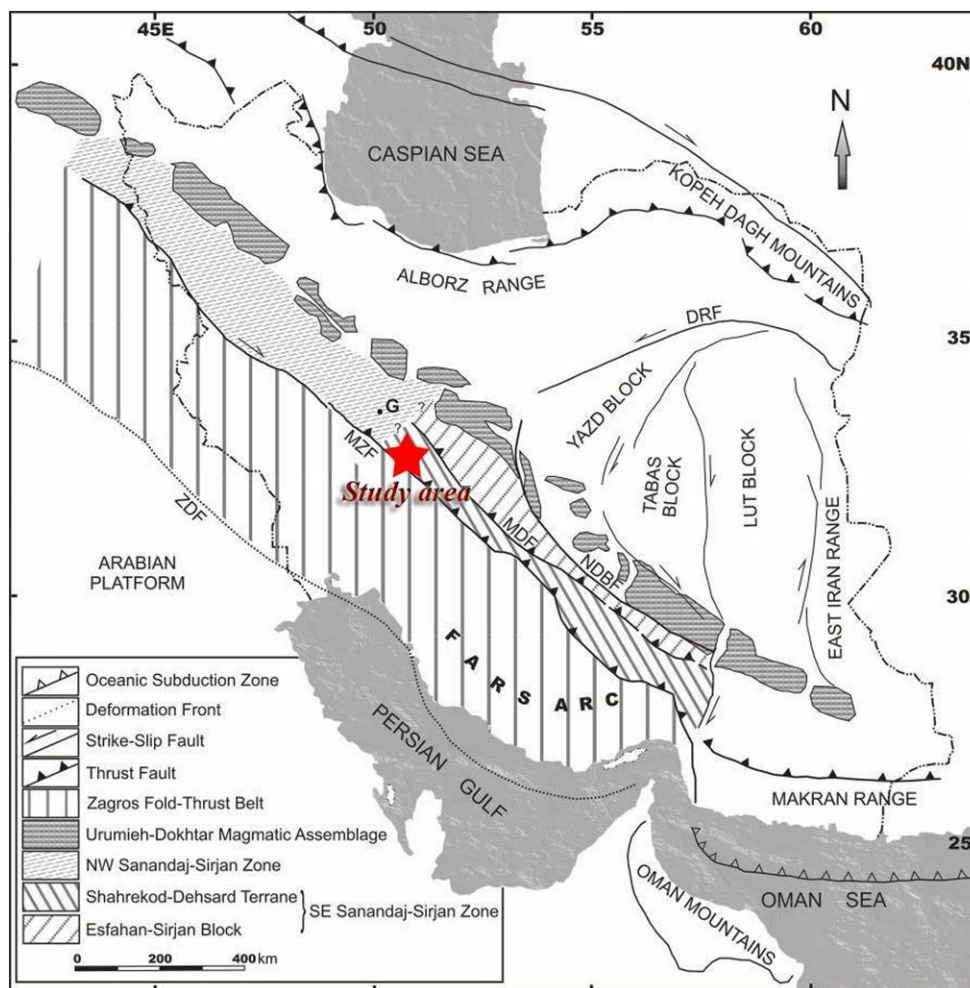




Fig. 1. Simplified structural map of Iran (compiled from [11]). DRF, Darouneh Fault; G, Golpaygan city; MDF, Main Deep Fault; MZF, Main Zagros Fault, NDBF, Naïen–Dehshir–Baft Fault; ZDF, Zagros Deformation Front.

**LEGEND**

Q	Quaternary: Alluvium
k	Cretaceous: Limestone
J2	Jurassic Shale and sandstone with interbedded limestone
J1	
Gn	Triassic-Jurassic :Gn (Green stone) was cut by Gs (meta alteration rocks and granitic intrusive)
	Road
	Village

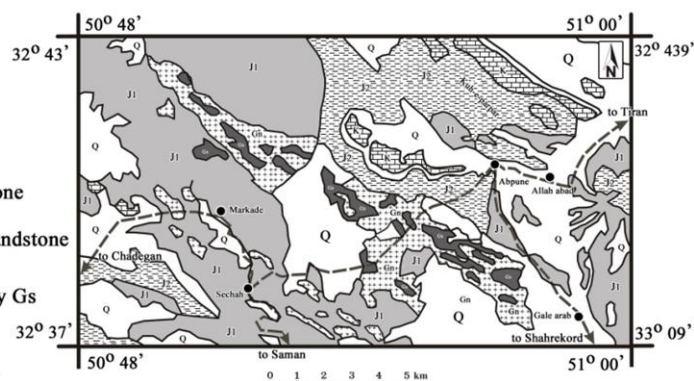


Fig. 2. Geological location of study area (modified from [11]).

### Geological setting

The study area belongs to Shahrekord-Dehsard terrain in the north western portion of Isfahan and is underlain by various rocks ranging in age from Triassic to Quaternary. This area is located 70 km NW of Isfahan, in central Iran (Fig. 1, 2). The lower most rock units in this area constitute Triassic-Jurassic metamorphosed igneous rocks which include meta basic rocks associated with greenschist and cut by doleritic dykes [14].

Jurassic sedimentary rocks consist of alternating shale and sandstone with interbedded limestone and dolomite (J1 and J2) which overlie metabasites and greenschists; contact is sharp but conformable [16]. These rocks developed over the greater part of the study area. Jurassic rocks are intruded by deformed granitoid bodies. This granite shows weaker metamorphic effects and become strongly deformed during subsequent deformation events [14]. Cretaceous rocks are represented by marine carbonate and terrigenous-carbonate facies which rest with an angular unconformity on Jurassic underlying rocks and crop out in the north-east of area [14-16].

### Sampling and Analytical techniques

A total of 68 relatively fresh samples were selected from the metabasites rocks of the study area. The samples were deformed and metamorphosed under at least greenschist facies conditions. As a result, metamorphic minerals replaced igneous minerals, and deformational fabrics are pronounced. Six samples after microscopic study, were analyzed for major, trace and rare earth elements (REE) in the ALS Chemex Analytical Laboratory (Vancouver, Canada) by using ICP-MS (inductively coupled plasma mass spectrometry) after acid decomposition (Table 1). Major elements were determined by ICP-MS

(inductively coupled plasma atomic emission spectrometry). Major element detection limits are about 0.001-0.2%. Four samples (A.13, A.16, A.20.B, and L.20) were analyzed for major and minor elements by X-ray fluorescence spectrometry at the Laboratory of Isfahan University, Iran.

### Petrography

The meta-magmatic rocks are metabasites and dolerite dykes. They crop out in the southern portion of Ab-Puneh Village. The meta-magmatic rocks are variably foliated. They are greenish in hand specimens due to a dominance of chlorite and green amphibole (Fig. 3a). They contain tremolite-actinolite, epidote, chlorite mineral paragenesis that is indicative of low-grade metamorphism.

Metabasites are mainly found in medium grained rocks, which commonly contain actinolitic amphibole, quartz, opaque minerals, and plagioclase porphyroblasts/phenocrysts (Fig. 3b). Also, these minerals along with other mineral phases variably constitute the groundmass. The amphibole schist samples do not show any relict minerals and contain trace plagioclase and recrystallized quartz aggregates in the groundmass. Plagioclase with lamellar twinning and amphiboles are the dominant phenocryst phases in the metabasalt and greenschist outside. In metabasalts, the igneous texture (ophitic/subophitic) and mineralogy (partially replaced pyroxenes, saussuritized plagioclase) are locally preserved. Also, completely replaced plagioclase and pyroxene are locally traceable in greenschists. Alterations are intense in some of the metabasite samples from shear zones. Secondary minerals include epidote, chlorite, carbonate and sericite.



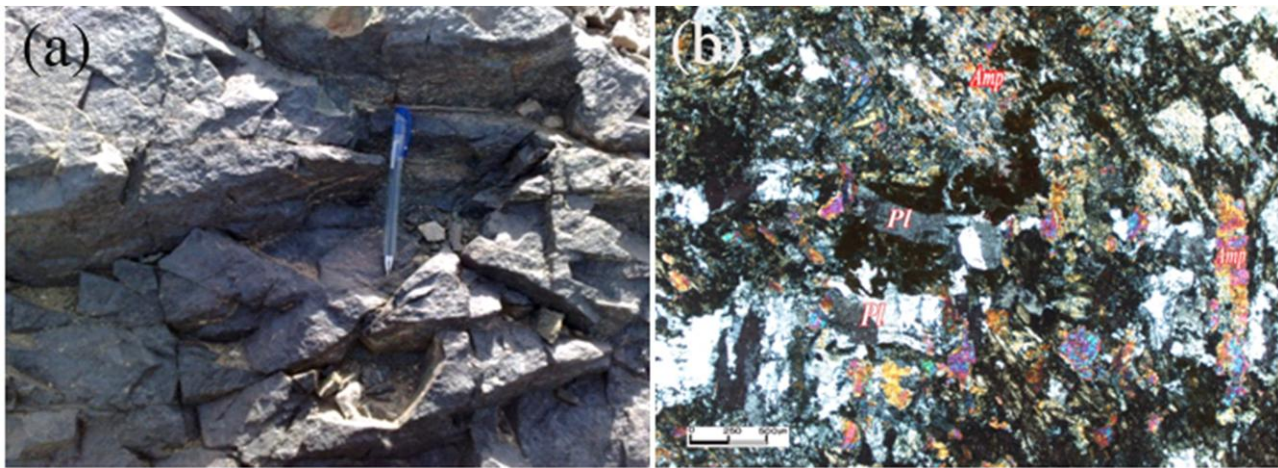


Fig. 3. Hand specimen (a) and microphotograph (b) of metabasites (Pl-plagioclase, Amp-amphibole)

Table.1 Major (Oxides: %wt) and trace elements (in ppm) data for metabasite rocks in study area

Sample	K5	K10	K12	K12-1	K18	K20	A.13	A.16	A.20.B	L.20
<b>Major elements (Wt %)</b>										
SiO <sub>2</sub>	44.2	51.7	46.7	45.4	46.2	48.5	50.091	46.78	54.54	45.071
Al <sub>2</sub> O <sub>3</sub>	14	15.55	14.4	14.5	16.85	14.9	10.83	15.49	14.1	14.37
Fe <sub>2</sub> O <sub>3</sub> T	17.7	13.15	14.35	14.95	10.3	12	11.98	10.96	7.72	10.131
CaO	9.82	7.58	10.85	10.8	9.27	9.82	10.14	10.32	4/93	9/121
MgO	6.12	2.55	6.66	6.15	10.55	6.42	6.162	3.138	9.291	8.674
Na <sub>2</sub> O	2.3	4.41	2.64	2.43	2.16	1.64	1.603	3.223	3/069	2/267
K <sub>2</sub> O	0.39	0.6	0.67	0.52	0.28	0.73	0.62	0.53	0/8	0/64
Cr <sub>2</sub> O <sub>3</sub>	0.03	0.13	0.06	0.08	0.83	0.06	.....	.....	.....	.....
TiO <sub>2</sub>	3.69	1.8	2.23	2.32	0.78	1.5	1.26	2.069	0/637	0/984
MnO	0.25	0.18	0.27	0.26	0.18	0.21	0.206	0.135	0/084	0/146
P <sub>2</sub> O <sub>5</sub>	0.19	0.74	0.2	0.07	0.1	0.17	0.215	0.378	0/212	0/233
SrO	0.02	0.04	0.04	0.04	0.03	0.02	.....	.....	.....	.....
BaO	0.01	0.02	0.03	0.02	0.01	0.01	.....	.....	.....	.....
LOI	1.77	1.46	1.55	2.25	2.36	2.37	6.58	6.67	5/020	8/40
<b>Total</b>	<b>100.49</b>	<b>99.91</b>	<b>100.65</b>	<b>99.79</b>	<b>99.9</b>	<b>98.4</b>	<b>99.687</b>	<b>99.693</b>	<b>100.603</b>	<b>99.674</b>
Zr/Nb	8.75	31.66	6.84	17.5	18.52	17.21	13.11	9.63	12.45	19
Zr/Y	2.03	3.06	2.09	1.49	3.42	3.21	3.28	3.21	7.61	3.96
La/Nb	0.8	4.21	1.29	1.83	1.74	1.31	0.44	0.63	0.27	1
Th/Ta	0.63	6.75	2.78	1.8	2.4	2.42	.....	.....	.....	.....
Th/Yb	0.1	0.61	0.56	0.11	0.315	0.27	.....	.....	.....	.....
Ta/Yb	0.165	0.09	0.2	0.065	0.13	0.11	.....	.....	.....	.....
Nb/Y	0.23	0.096	0.31	0.85	0.185	0.186	0.25	0.33	0.61	0.21
Th/La	0.059	0.13	0.15	0.082	0.1	0.12	0.75	0.4	0.33	0
Ti/Zr	632.04	70.99	230.5	662.3	93.52	85.64	.....	.....	.....	.....
Mg#	40.9	28.07	48.11	45.16	67.17	51.61	.....	.....	.....	.....
FM	0.49	0.6	0.42	0.45	0.25	0.38	.....	.....	.....	.....

Table.1 (continue)

Sample	K5	K10	K12	K12-1	K18	K20	A.13	A.16	A.20.B	L.20
<b>Trace elements (ppm)</b>										
Au	<0.001	<0.001	<0.001	<0.001	<0.001	0.007				
Ag	<1	<1	<1	<1	<1	<1				
Ba	101.5	174	257	173	111.5	118.5	114	174	133	210
Co	51.3	19.7	30.5	32.7	53.1	41.9	46	28	29	42
Cr	210	900	430	570	5960	430	239	200	172	285
Cs	0.48	0.22	0.51	0.47	1.2	0.5				
Cu	48	14	21	25	69	114	91	62	5	53
Ga	19.9	26.2	20.5	18.5	15.3	18.3				
Hf	1	3.9	1.8	0.7	1.4	3				
Mo	<2	2	<2	<2	<2	<2				
Nb	4	4.8	8.6	1.2	2.7	6.1	9	8	11	5
Ni	24	11	76	33	186	51	49	9	39	157
Pb	9	10	12	11	26	20	29	46	13	15
Rb	11.1	12.3	13.1	10	7	34.7	30	18	33	28
Sn	<1	3	1	<1	1	1				
Sr	188.5	312	331	278	207	167	184	285	266	254
Ta	0.3	0.4	0.6	0.1	0.2	0.4				
Th	0.19	2.7	1.67	0.18	0.48	0.97	3	2	1	0
Tl	<0.5	<0.5	<0.5	<0.5	<0.5	<0.5				
U	0.1	0.99	0.79	0.08	0.14	0.36	4	5	9	3
V	675	129	366	417	150	288	243	229	239	143
W	3	2	3	2	2	1				
Y	17.2	49.7	27.7	14.1	14.6	32.7	36	24	18	24
Zn	161	100	176	170	294	1040	1438	605	189	289
Zr	35	152	58	21	50	105	118	77	137	95
<b>Rare elements (ppm)</b>										
La	3.2	20.2	11.1	2.2	4.7	8	4	5	3	5
Ce	7.9	46.5	23.7	5.6	10.8	18.8				
Pr	1.27	6.64	3.18	0.93	1.54	2.85				
Nd	6.9	30.5	13.8	4.9	7.2	13.4				
Sm	2.22	7.94	3.68	1.66	1.96	3.86				
Eu	1.3	2.75	1.59	1.21	0.91	1.44				
Gd	2.74	9.04	4.31	2.03	2.37	4.68				
Tb	0.53	1.56	0.81	0.42	0.43	0.93				
Dy	3.44	9.29	5.33	2.88	2.77	6.42				
Ho	0.73	1.97	1.07	0.59	0.58	1.3				
Er	2.04	5.32	3.08	1.69	1.56	3.74				
Tm	0.28	0.74	0.45	0.24	0.26	0.54				
Yb	1.81	4.41	2.96	1.53	1.52	3.6				
Lu	0.27	0.69	0.43	0.24	0.22	0.54				

### Bulk sample geochemistry

Results of whole-rock geochemical analysis of all samples are presented in Table 1. The metabasite samples display SiO<sub>2</sub>, Al<sub>2</sub>O<sub>3</sub>, K<sub>2</sub>O and MgO contents ranging from 44.2 to 54.54, from 14 to 16.85, from 0.28 to 0.8 and from 2.55 to 10.55 wt% respectively. The metabasite rocks are basic to intermediate in composition with SiO<sub>2</sub> %wt ranging from 44.2 to 54.54. However, most samples have SiO<sub>2</sub> below 51% and high MgO (>6%) indicating the predominance of modestly fractionated basalts in the series. On the base of geochemical diagrams, Zr/TiO<sub>2</sub> \*10<sup>-4</sup> vs. Nb/Y

diagram [17] (Fig. 4a), the samples plot in the basalt field of this diagram. They show a low Nb/Y ratio indicating subalkaline affinities (Fig.4b). This diagram is preferred to the more commonly used total-alkali-silica (TAS) classification diagram [18] as there may have been mobility of K in some of the more altered samples. The total alkali content is low and K<sub>2</sub>O is lower than Na<sub>2</sub>O indicating a low-K and Fe-enriched tholeiitic nature. Tholeiitic trend is clearly indicated on the AFM diagram (Fig. 5a). Na<sub>2</sub>O+K<sub>2</sub>O vs. Al<sub>2</sub>O<sub>3</sub> diagram [19]; the metabasite is dominated by sub-alkaline tholeiitic affiliation with moderate to high-Al basalts (Fig. 5b).

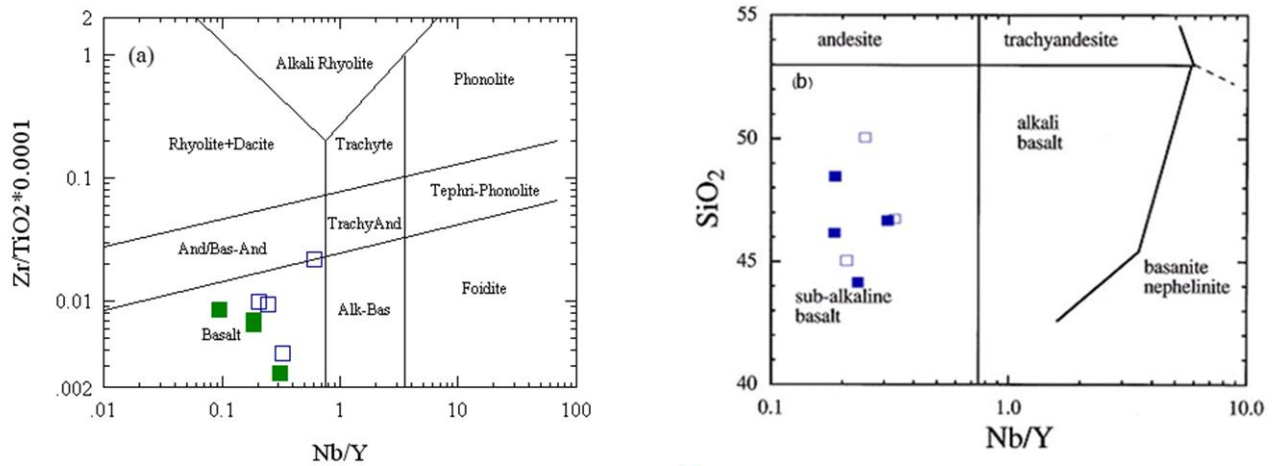


Fig. 4. Classification of magma types (a),  $Zr/TiO_2 * 10^{-4}$  vs. Nb/Y diagram [17] for metabasite.  $SiO_2$  versus Nb/Y [18]. (■ ICP-MS samples & □ X-ray samples)

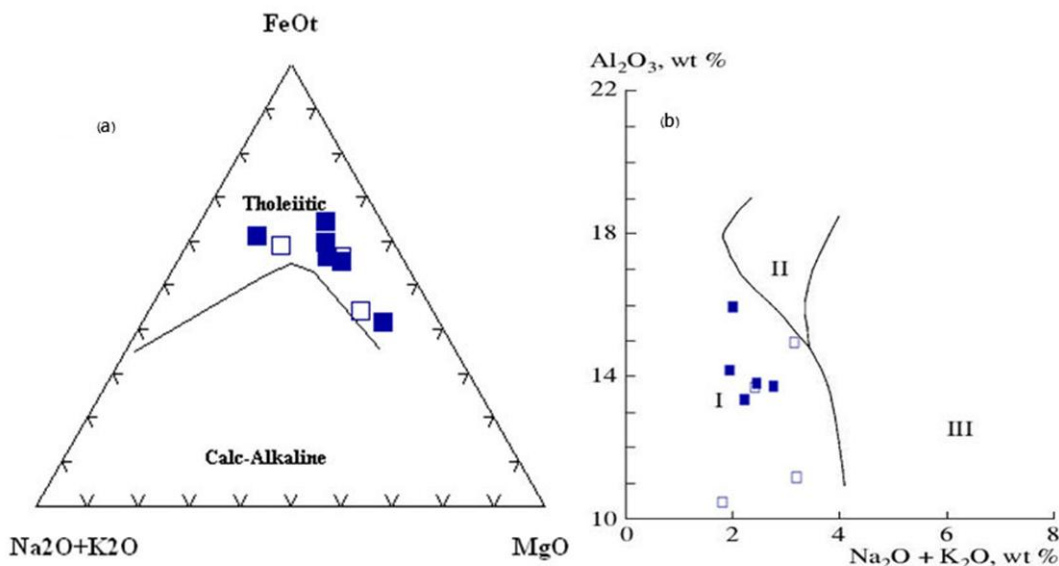


Fig. 5. The metabasite samples plot in sub-alkaline field. Classification of the studied rocks on (a) AFM [19], (b)  $Na_2O+K_2O$  vs  $Al_2O_3$  diagram [20] for the metabasite rocks. Fields: I-tholeiitic, II-aluminous basalts, III-alkaline basalts. Symbols are the same as in Fig. 3.

### Trace and rare earth elements (REEs)

In general, the chondrite normalized REE patterns of all metabasite rocks are characterized by moderate to high LREE enrichment [ $(La/Yb)_N = 1.17-3.05$ ] and unfractionated HREE [ $(Gd/Yb)_N = 1.04-1.63$ ]. The metabasite rocks exhibit similar chondrite-normalized and primitive mantle-normalized REE patterns (Fig. 6a and b). The E-MORB normalized spider diagrams of the metabasite rocks were more similar to E-MORB (Fig. 6c). The Oceanic Island Basalt normalized patterns of these rocks are characterized by moderately fractionated REE with enrichment in HREE and depletion in LREE. (Fig. 6d).

Sampling rocks are normalized to Chondrite and primitive mantle [21], (Fig. 7a,b) Rocks are enriched in

LILE (e.g., Ba and Pb), relatively depleted in HFSE (e.g., Ni, Ti). Well-defined negative anomaly is observed for Ni. Fractionation or presences of some minerals in the restates explain the negative anomalies, for example, olivine (Ni) and limonite and/or titanite (Ti). normalized to an average E-type MORB composition of the metabasite, show similarities and most of the samples have upper HFSE and LILE contents than Oceanic Island Basalt [23], Fig. 7.c.d). Metabasites have high Ba/Nb ( $> 28$ ) ratios which is a common feature of arc magmas (e.g. [24]) and high La/Nb ratios (0.27-4.21) indicating crustal involvement [25]. Further, prevalent low Ce/Pb and Rb/Ba values also suggest lithospheric contributions.

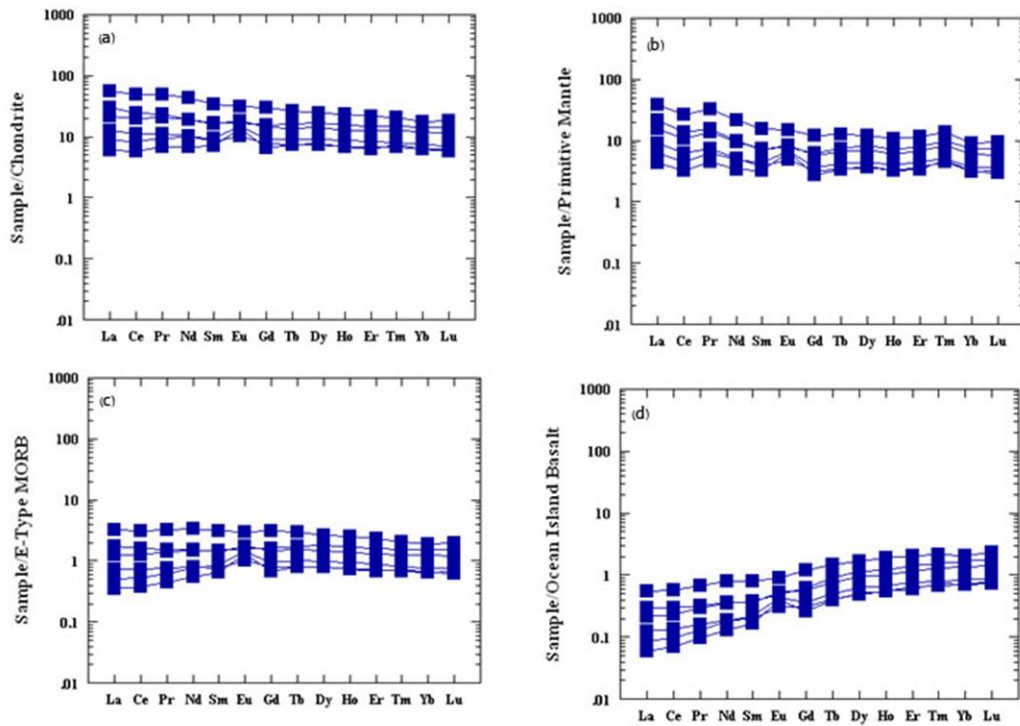


Fig.6. (a) Chondrite-normalized REE pattern for metabasite rocks. (b) The metabasite rocks normalized with primitive mantle, Normalization data from [21]. (c) E-type MORB-normalized. (d) Oceanic Island Basalt (normalized data from [22]).

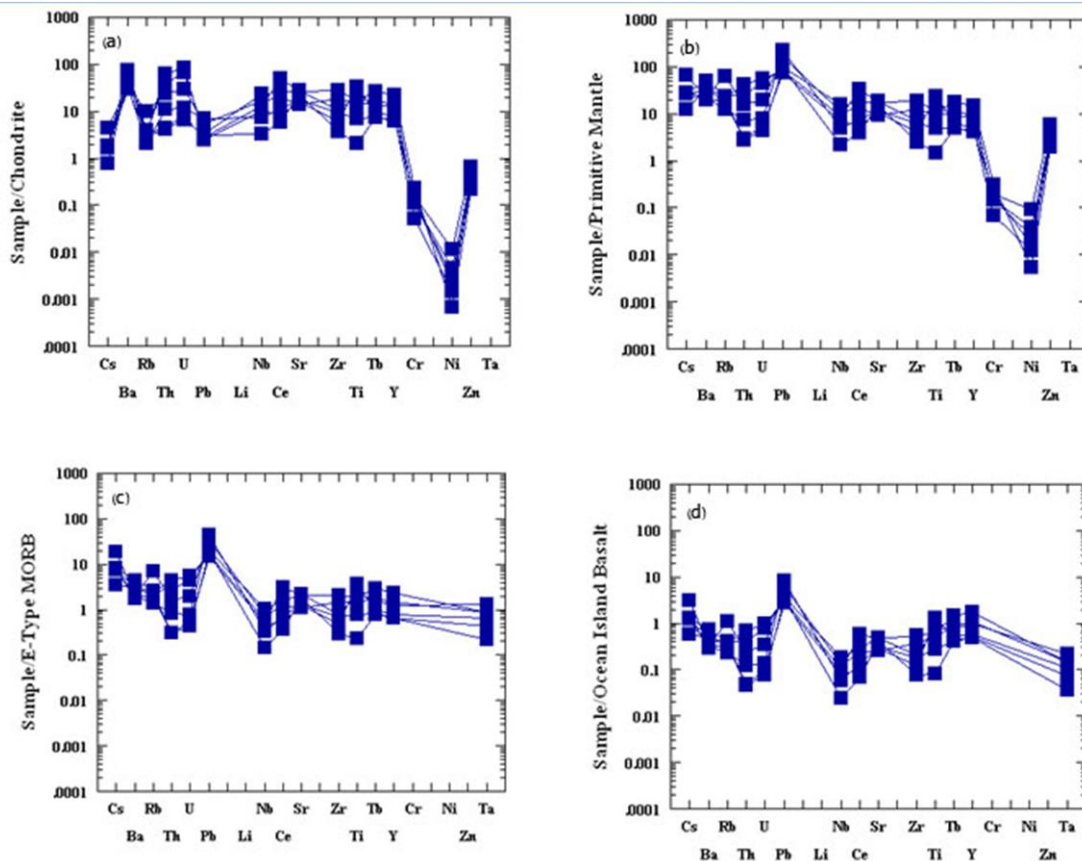


Fig.7. Plate trace elements pattern. (a) Chondrite-normalized.(b) primitive mantle (normalized data from [21]), (c) E-type MORB-normalized .(d) Oceanic Island Basalt (normalized data from [22]).

### Tectonic setting

Tectonic discrimination on Y, Zr and Ti triangular diagram [30] shows that most sample plot on the ocean floor basalt fields (Fig. 8a).

The  $\text{CaO}/\text{TiO}_2$  and  $\text{Al}_2\text{O}_3/\text{TiO}_2$  ratios for the basic rocks from the metabasites are shifted towards lower values than most volcanic arc rocks (Fig. 8b) suggesting a source that is not similar to the source for the modern arc lavas [26]. Wilson [27] has indicated that a contribution from the subducted component in terms of the highly incompatible elements such as Ti, Zr, Y and Nb is insignificant compared to the role from the asthenospheric mantle wedge above the subducted slab. Besides, the higher ratios of the incompatible elements with respects to average basalts from oceanic island-arcs and normal mid-oceanic ridges may

indicate a contribution from an incompatible elements-enriched melt.

Within-plate basalts having higher Ti/Y and higher Nb/Y reflect an enriched mantle source relative to the source of MORB and volcanic arc basalts [22], the analyzed rocks plot in the plate-margin basalts, indicating enrichment in Zr and Ti compared with Within-plate basalts (Fig. 8c). Zr/Y plotted against the fractionation index Zr (adapted from [28]) provided an effective discrimination between the basalts from ocean-island arcs, mid-ocean basalts, within-plate basalts and back-arc basin basalts [22], and the metabasite plot in the field of back-arc basin basalts (Fig. 8d). Back-arc basin basalts (BABB) have notably higher Zr, lower Ti/Zr, V/Ti and Sc/Y values than island arc basalts (IAB) [29].

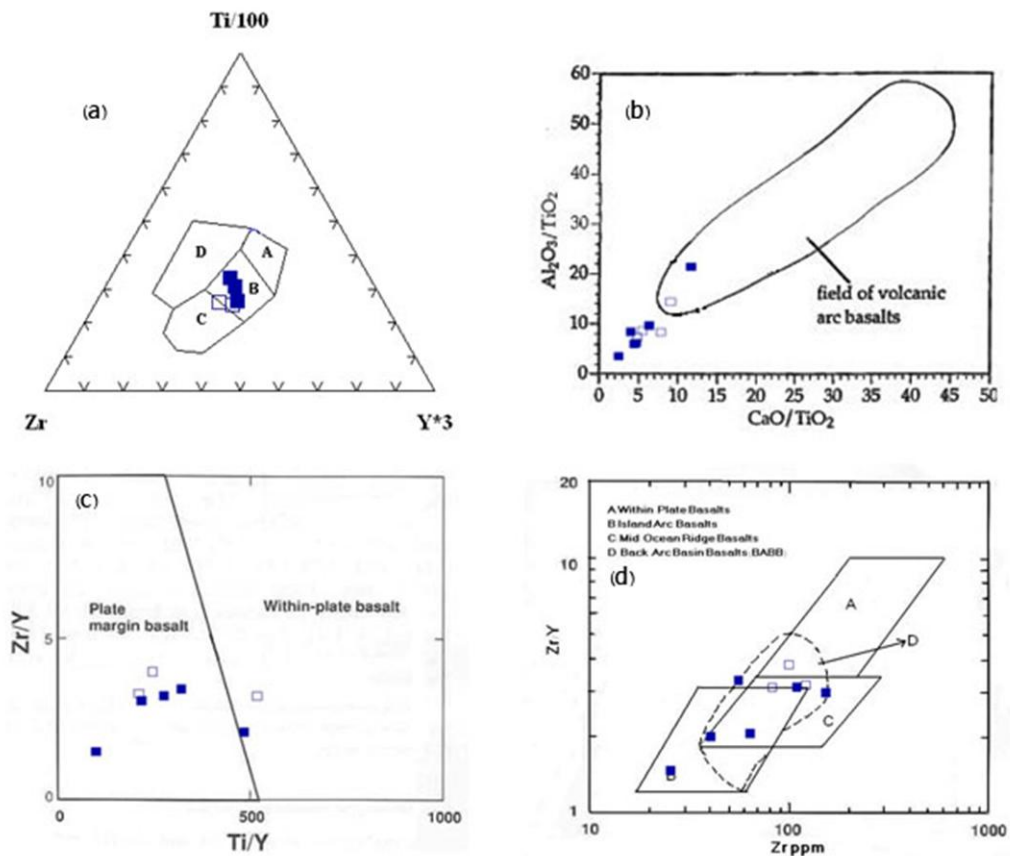


Fig. 8. tectonic discrimination diagrams for metabasite on (a) Ti/100-Zr-3Y [30]. Tectonic discrimination on Y, Zr and Ti triangular diagram shows that most samples plot on the ocean floor basalt field, (b) Plots of the metabasite rocks on  $\text{CaO}/\text{TiO}_2$  versus  $\text{Al}_2\text{O}_3/\text{TiO}_2$  diagram [26]. (c) Zr/Y-Ti/Y diagram [31]. (d) Zr/Y-Zr diagram [28]; back-arc basalts discrimination from [32]. Symbols are the same as in Fig. 3.

A: island arc basalts, B: ocean floor basalts, C: calc-alkaline basalts, D: within plate basalts.

### Discussions and conclusions

The Sanandaj-Sirjan Zone is thrust over the Arabian platform along the main Zagros Fault [32-33]. The main Zagros Fault is deeply rooted and coincides

with the suture between the Arabian plate and Sanandaj-Sirjan Zone [6-7]. The main ambiguity on the tectonic evolution of the southeastern Zagros orogenic belt is the time when the Neo-Tethys oceanic crust disappeared completely between the central Iran



Microcontinent and the Arabian Plate [35-36]. Based on this review, the subduction of the Neo-Tethys oceanic lithosphere has continued up to middle Miocene time and final collision between the Arabian plate and the central Iran microcontinent occurred in the late micro continent [37]. Once Neo-Tethys rifting occurred in the upper Carboniferous- lower Permian [38]. In the upper Triassic- lower Jurassic Neo-Tethys underthrust under the central Iran microcontinent [34]. Arfania and Shahriari[35] have suggested that Shahrekord-Dehsard consists of two oceanic basins, Neo-Tethys 1 and Neo-Tethys 2. This model shows the evolution in several stages, Subduction, Oceanic lithosphere and continental collision of upper Triassic to Pliocene. During the late Triassic- early Jurassic a new spreading ridge, the second Neo-Tethys, was created to separate the Shahrekord-Dehsard terrain from the Afro- Arabian plate and developed back arc basin. Simultaneously, the second Neo-Tethys spreading and primary Neo-Tethys closing occurred in the upper Miocene and late ? Most likely the upper Miocene- Pleistocene, second Neo-Tethys is completely closed. According to this research, metabasites in the study area are of basaltic composition with sub-alkaline and tholeiitic trends, indicated to the oceanic crust and were created in a back arc basin environment. Chemically these rocks are as much enriched as N-type MORB and similar E-type MORB. Metabasite rocks are probably remnants of the second Neo-Tethyan Oceanic crust with a back arc basin environment. Arfania and Shahriari[35] have showed that most likely, rifting and spreading jumped west to separated Shahrekord-Dehsard terrane from the north-eastern margin of the Afro-Arabian continent, creating the new Neo-Tethys(equal Neo-Tethys 2) in Trassic- Jurassic time. This new plate was probably active by the end of Mesozoic time. I suggest that because of their petological and geochemical nature, metabasites represent relics of the Neo-Tethys oceanic plate, which was subducted under the Iranian microcontinent (as a part of Eurasia). Such an interpretation is in agreement with Arfania and Shahriari [35], Davoudian et al. [15], Gasemi and Talbot [39], Sepehr and Cosgrove[40] and Mohajjel et al. [4].

## References

- [1] Alavi M., 2004. Regional stratigraphy of the Zagros fold-thrust belt of Iran and its proforeland evolution. *American Journal of Science*. 304, p. 1-20.
- [2] Mohajjel, M., and Fergusson, C. L., 2000. Dextral transpression in Late Cretaceous continental collision, Sanandaj - Sirjan zone, Western Iran. *Journal of Structural Geology*, vol. 22 (8), p. 1125 - 1139.
- [3] Sengor, M.C., and Natalin, B.A., 1996. Paleotectonics of Asia: Fragments of a synthesis. In Yin A. & Harrison T. M. (eds.) *The Tectonic Evolution of Asia*, p. 486-640, Cambridge University Press, Cambridge.
- [4] Mohajjel, M., Fergusson, C.L., Sahandi, M.R., 2003. Cretaceous-Tertiary convergence and continental collision, Sanandaj-Sirjan Zone, Western Iran. *Journal of Asian Earth Sciences*, vol.21, p. 397-412.
- [5] Ricou, L.E., 1974. L'étude géologique de la région de Neyriz (Zagros iranien) et l'évolution des Zagrides. Thesis, Université Paris-Sud, Orsay.
- [6] Agard, P., Omrani, J., Jolivet, L., and Mouthereau, F., 2005. Convergence history across Zagros (Iran): Constraints from coalitional and earlier deformation. *International Journal of Earth Sciences*, vol.94, p.401-19.
- [7] Berberian, M., 1995. Master 'blind' thrust faults hidden under the Zagros folds: Active basement tectonics and surface morphotectonics. *Tectonophysics*, vol.241, p.193-224.
- [8] Mouthereau, F., Tensi, J., Bellahsen, N., Lacombe, O., De Boisgollier, T., and Kargar, S., 2007. Tertiary sequence of deformation in a thin-skinned/thick-skinned collision belt: The Zagros Folded Belt (Fars, Iran). *Tectonics* 26, TC5006 doi: 10.1029/2007TC002098.
- [9] Eftekharnjad, J., 1981. Tectonic division of Iran with respect to sedimentary basins. *Journal of Iranian Petroleum Society*, vol.82, p. 19-28 (in Farsi).
- [10] Taraz, H., 1974. Geology of the Surmogh-Deh Bid Area, Abadeh Region, Central Iran. Report (37). Geological Survey of Iran, Tehran.
- [11] Gasemi, A., Hosaini, M., 2007. 1:100000 Geological map of Chadegan. Geological survey and mineral explorations of Iran.
- [12] Alavi, M., 1994. Tectonics of the Zagros Organic belt of Iran: New Data & Interpretations *Tectonophysics*, v.229, p.211-238.
- [13] Davoudian, A.R., Khalili, M., Noorbehesht, I., Mohajjel, M., 2005. The tectonometamorphic & magmatic evolution in the Shahrekord- Daran area (Sanandaj-Sirjan Zone, Iran). Ph.D. thesis. University of Isfahan. 217 p.
- [14] Nasr-Esfahani, A.K., Hamid Reza Ziaei, H.R., 2007. Using multivariable statistical methods to separation and detection of lithologic units in ETM<sup>+</sup> satellite images, case study: outcrops in the south of Ab-Poneh village, Tiran (west Isfahan), *JSAU*, vol.17, No.65, p.27-42.
- [15] Davoudian, A.R., Genser, J., Dachs, E., Shahanian, N., 2008. Petrology of eclogites from north of Shahrekord, Sanandaj-Sirjan zone, Iran.
- [16] Eliasi, N., Emami, N., Nasr-Esfahani, A.K., Vahabi Moghaddam, B., 2011. Mineralogy and determination of tectonomagmatic setting of subvolcanic rocks in North of Shahrekord by using clinopyroxene mineral chemistry, Vol. 19, No.2, p. 207-218.
- [17] Winchester, J.A., and Floyd, P.A., 1977. Geochemical discrimination of different magma series and their differentiation products using immobile elements. *Chemical of Geology*, vol.20, p. 325-343.
- [18] Le Bas. M.J., Le Maitre, R.W., Streckeisen, A., Zanetin, B., 1986. A chemical classification of volcanic rocks based on the total alkalis-silica diagram. *J. Petrol.*, vol.27, p. 745-750.
- [19] Irvine, T.N., Baragar, W.R.A., 1971. A guide to the chemical classification of the common volcanic rocks. *Canadian Journal of Earth Science* 8. pp. 523-548.
- [20] Kuno, H., 1961. High Alumina Basalt. *Journal of petrology*, vol.1, p. 121-145.
- [21] Taylor, S.R., McLennan, S.M., 1985. *The Continental Crust: its Composition and Evolution*. Blackwell,

- Cambridge. 312 p.
- [22] Rollinson, H., 1993. Using geochemical data: evaluation, presentation, interpretation. Longman Scientific and Technical., 352 p.
- [23] Sun, S.S., McDonough, W.F., 1989. Chemical and isotopic systematic of oceanic basalts: implication for mantle composition and processes. In: Sunders, A.D., Norry, M.J. (Eds.), *Magmatic in Oceanic Basins*, Special Publication. 42. Geology Society of London, p. 313–345.
- [24] Fitton, J.G., James, D., Leeman, W.P., 1991. Basic magmatism associated with late Cenozoic extension in the western United States: compositional variations in space and time. *Journal of Geophysical Research* 96, pp. 13693-13711.
- [25] Hasse, K.M., Muhe, R., Stoffers, P., 2000. Magmatism during extension of the lithosphere: geochemical constrains from lavas of the Shaban deep. Northern Red Sea. *Chemical geology* 166, p. 225-239.
- [26] Sun, S.S., Nesbitt, R.W., 1978. Geochemical regularities and genetic significance of ophiolitic basalts. *Geology* 6, p. 689-693.
- [27] Wilson, M., 1989. *Igneous Petrogenesis*. Unwin Hyman, London, p. 11in
- [28] Pearce, J.A., and Norry, M.J., 1979. Petrogenetic implication of Ti, Zr, Y and Nb variation in volcanic rocks. *Contribution to Mineral and Petrology*, vol.69, p. 33-47.
- [29] Woodhead, J., Eggins, S., and Gamble, J., 1993. High field strength and transition element system in island arc back-arc basin basalts: evidence for multi-phase melt extraction and depleted mantle wedge. *Earth and Planetary Science Letters*, vol. 114, p. 491-504.
- [30] Pearce, J.A., Cann, J.R., 1973. Tectonic setting of basic volcanic rocks determined using trace element analyses. *Earth and Planetary Science Letters*, vol.19, p. 290-300.
- [31] Pearce, J.A., and Gale, G.H., 1977, Identification of ore deposition environment from trace element geochemistry of associated igneous host rocks. In *Volcanic Processes in Ore Genesis* (ed. M. J. Norry), Geological Society of London, vol.7.
- [32] Floyd, P.A., Kelling, G., Gokcen, S.L and Gokcen, N., 1991. Geochemistry and tectonic environment of basaltic rocks from the Misis ophiolitic mélange, south Turkey. *Chemical Geology*, 89. p. 263-80.
- [33] Shahabpour, J., 2007. Island-arc affinity of the Central Iranian Volcanic Belt. *Journal of Asian Earth Sciences*, vol.30, p. 652–65
- [34] Reuter, M., Piller, W.E., Harzhauser, M., et al. 2007. The Oligo-/Miocene Qom Formation (Iran): Evidence for an early Burdigalian restriction of the Tethyan Seaway and closure of its Iranian gateways. *International Journal of Earth Science*, vol.98, p.627–50 doi: 10.1007/s00531-007-0269-9.
- [35] Arfania, R., Shahriari, S., 2009. Role of southeastern Sanandaj-Sirjan Zone in the tectonic evolution of Zagros Orogenic Belt, Iran. *Journal of Island Arc*, vol.18, p. 555–576.
- [36] Fakhari, M.D., Axen, G. J., Horton, B. K., Hassanzadeh, J., and Amini, A., 2008. Revised age of proximal deposits in the Zagros foreland basin and implications for Cenozoic evolution of the High Zagros. *Tectonophysics*, 451, 170–85 doi: 10.1016/j. tecto. 2007. 11.064.
- [37] Babaie, H.A., Ghazi, A.M., Babaei, A., Duncan, R., Mahony, J., and Hassanipak, A., 2003. New Ar-Ar age, isotopic, and geochemical data for basalts in the Neyriz ophiolite, Iran. *Geophysical Research Abstracts* 5, 12 899.
- [38] Shafaii-Moghadam, H., Rahgoshay, M., and Whitechurch, H., 2007. The Naien-Baft ophiolites: An evidence of back-arc basin spreading in the active margin of the Iranian continent. *Geophysical Research Abstracts*, vol.9, 791 p.
- [39] Ghasemi A., Talbot, C. J. 2006. A new tectonic scenario or the Sanandaj-Sirjan Zone (Iran). *Journal of Asian Earth Sciences* vol.26, p. 683–93.
- [40] Sepehr, M., Cosgrove, J.W., 2004. Structural framework of the Zagros Fold-Thrust Belt, Iran. *Mar Petrol. Geol.* 21, p. 829-843.